Minimum Noise Figure of the Variable-Capacitance Amplifier

By K. KUROKAWA and M. UENOHARA

(Manuscript received November 2, 1960)

The variable-capacitance diode is one of the most promising nonlinear elements for low-noise parametric amplifiers. In practice, however, these diodes have a small series resistance, and this limits the minimum obtainable noise figure; for the better diodes, the effect of the shunt conductance can be neglected. Taking the contribution of this series resistance into account, this paper discusses the minimum noise figure of parametric amplifiers under various conditions. It is shown that the minimum noise figures are basically determined by a dynamic quality factor of the diode, which will be defined in this paper, under the assumed model of a series resistance as the only parasitic element. Identical minimum noise figures are obtained for lower sideband amplifiers operated with optimum idler frequency, for those with the idler load at 0°K, and for the upper sideband up-converter. In terms of the over-all systems noise figure, however, the lower sideband amplifier is superior to the upper sideband up-converter, for here the gain is limited by the ratio of output to input frequency.

Experimental values are given for the figure of merit of various diodes. Universal curves are also given which demonstrate noise behavior of the various systems as a function of the network parameters and component temperatures.

I. INTRODUCTION

The variable-capacitance parametric amplifier is of interest primarily because it shows promise of very low noise amplification. However, variable capacitance diodes have a small but finite series resistance which limits the obtainable minimum noise figure; for the better diodes, the shunt conductance can be neglected.

Taking the contribution of this resistance into account, Leenov[1] has discussed the noise figure of upper sideband up-converter, and Haus and Penfield[2] and others[3,4,5] have discussed the lower sideband circulator-type amplifier. This paper discusses the lower sideband idler output

amplifier and the degenerate amplifier, in addition to the amplifiers mentioned above, and compares them to one another. Further, we shall demonstrate the unique importance of the dynamic quality factor $\tilde{Q}$, as defined here, in characterizing the diode at a given temperature for noise figure considerations.

The diode is assumed to be a series connection of a junction capacitance $C(t)$, which is a periodic function of time, and a spreading resistance R_s.

Leenov, as well as Haus and Penfield, used the open-circuit assumption for the unwanted frequencies at the diode junction. However, there are a number of published papers[3,5,6,7,8] in which the short-circuit assumption is used. We shall discuss both of these cases simultaneously, and show that the two assumptions give the same expressions for the noise figure, if the dynamic quality factor $\tilde{Q}$ is redefined for each case.

The following conclusions are obtained:†

(a) The noise figure of a diode amplifier is basically determined by the dynamic quality factor $\tilde{Q}$ of the diode; the noise figure improves with increasing value of $\tilde{Q}$.

(b) The minimum noise figure for room temperature operation of the lower sideband amplifiers is obtained when the idler load resistance approaches zero.

(c) For a given $\tilde{Q}$ at the signal frequency, there exists an optimum idler frequency which gives the smallest noise figure for the particular diode.

(d) Refrigeration of the idler load improves the noise figure only under certain conditions. As long as the idler frequency is lower than the optimum, the noise figure of the amplifier with an idler load at zero temperature absolute can be as low as that obtained using the optimum idler frequency.

(e) The minimum noise figure of the upper sideband up-converter is equal to that of the lower sideband amplifiers with the optimum idler frequency or with a zero temperature idler load.

The conclusions (b) and (c) are similar to those reached by Haus and Penfield,[2] Kotzebue,[4] and Knechtli and Weglein,[5] but are extended in this paper to include the case of lower sideband idler output amplifiers. In this case, to obtain the minimum noise figure, most of the idler power generated by the parametric action is to be dissipated in the series resistance of the diode. The output power, however, can be finite because of the unlimited gain obtainable with the negative resistance effect.

† Similar conclusions have been obtained by R. P. Rafuse of M.I.T. (private communication).

The conclusion (e) states further that, if the same diode is to be employed, a superior over-all noise figure performance is obtained with the lower sideband amplifier, inasmuch as the gain of the lower sideband amplifier can be larger than that of the upper sideband one. Nevertheless, there are other significant applications of the upper sideband upconverter which make its study important.

Two aspects of minimum noise amplification, not covered in the literature, are discussed in detail. These are

(a) the effects of load refrigeration;

(b) optimum upper sideband construction.

Universal curves are included which demonstrate noise behavior of the various systems as a function of $\tilde{Q}$.

II. EQUIVALENT CIRCUIT OF THE LOWER SIDEBAND AMPLIFIER

If the assumption is made that the only currents which flow through the diode junction are at the signal (ω_1) and idler (ω_2) frequencies, that is, making the open-circuit assumption for the unwanted frequencies, the junction is characterized by the following equation:

$$\begin{bmatrix} e_1 \\ e_2^* \end{bmatrix} = \begin{bmatrix} \dfrac{1}{j\omega_1 K_0} & -\dfrac{1}{j\omega_2(2K_1)} \\ \dfrac{1}{j\omega_1(2K_1)} & -\dfrac{1}{j\omega_2 K_0} \end{bmatrix} \begin{bmatrix} i_1 \\ i_2^* \end{bmatrix}, \tag{1}$$

where e is the junction voltage, i is the junction current, and their subscripts 1 and 2 refer to the signal (ω_1) and idler (ω_2) frequencies respectively.

The quantities K_0 and K_1 are defined by

$$\frac{1}{C(t)} = \frac{1}{K_0} + \frac{1}{K_1}\cos \omega_p t + \cdots, \tag{2}$$

where $C(t)$ is a junction capacitance which is a periodic function of time.

If, on the other hand, the assumption is made that the only voltages which appear across the junction are at the signal and idler frequencies, that is, making the short circuit assumption for the unwanted frequencies, the junction is characterized by

$$\begin{bmatrix} i_1 \\ i_2^* \end{bmatrix} = \begin{bmatrix} j\omega_1 C_0 & -j\omega_1 \dfrac{C_1}{2} \\ j\omega_2 \dfrac{C_1}{2} & -j\omega_2 C_0 \end{bmatrix} \begin{bmatrix} e_1 \\ e_2^* \end{bmatrix}, \tag{3}$$

where C_0 and C_1 are defined by

$$C(t) = C_0 - C_1 \cos \omega_p t + \cdots . \tag{4}$$

If both sides of (3) are multiplied by the inverse of the two-by-two matrix, (3) becomes

$$\begin{bmatrix} e_1 \\ e_2^* \end{bmatrix} = \begin{bmatrix} \dfrac{C_0}{j\omega_1\left(C_0^2 - \dfrac{C_1^2}{4}\right)} & -\dfrac{\dfrac{C_1}{2}}{j\omega_2\left(C_0^2 - \dfrac{C_1^2}{4}\right)} \\ \dfrac{\dfrac{C_1}{2}}{j\omega_1\left(C_0^2 - \dfrac{C_1^2}{4}\right)} & -\dfrac{C_0}{j\omega_2\left(C_0^2 - \dfrac{C_1^2}{4}\right)} \end{bmatrix} \begin{bmatrix} i_1 \\ i_2^* \end{bmatrix}. \tag{5}$$

The diagonal terms in the impedance matrices of (1) and (5) are just ordinary capacitances in series with the variable capacitance and, therefore, play no essential role in the parametric process. These capacitances are included in the input and output circuits, which are expressed by the impedances Z_{11} and Z_{22} respectively.

The series resistance R_s is considered as the only dissipative element of the diode,† and the dynamic quality factor of the diode is defined by

$$\tilde{Q} = \frac{1}{\omega \mid 2K_1 \mid R_s}$$

(for open-circuit assumption), (6)

$$\tilde{Q} = \frac{\dfrac{\mid C_1 \mid}{2}}{\omega \left| C_0^2 - \dfrac{C_1^2}{4} \right| R_s} = Q_0 \frac{1}{\left(\dfrac{2}{\gamma} - \dfrac{\gamma}{2}\right)}$$

(for short-circuit assumption) (7)

respectively, where‡

$$\gamma = \frac{\mid C_1 \mid}{C_0} \tag{8}$$

and Q_0 is the ordinary quality factor of the diode defined by

$$Q_0 = \frac{1}{\omega C_0 R_s} . \tag{9}$$

† For low-noise gallium arsenide diodes this assumption is good up to X-band, but for silicon mesa-type diodes a shunt conductance has to be taken into account at frequencies around this band.

‡ Our γ is twice the γ used by Kotzebue.[4]

If $C(t)$ is sinusoidal, an expression for the dynamic quality factor for the open-circuit assumption can be obtained in terms of γ and Q_0 :

$$\tilde{Q} = Q_0 \frac{1 - \sqrt{1 - \gamma^2}}{\gamma \sqrt{1 - \gamma^2}}. \tag{10}$$

When γ is small, the dynamic quality factor simplifies to

$$\tilde{Q} = \frac{\gamma}{2} Q_0 \tag{11}$$

for both assumptions, but when γ approaches unity, the open-circuit assumption gives a larger value for $\tilde{Q}$, as shown in Fig. 1.

If, on the other hand, $1/C(t)$ is sinusoidal, the same value of $\tilde{Q}$ is obtained for both short- and open-circuit assumptions.

Using these two definitions of the dynamic quality factor, the same equivalent circuit is obtained for both assumptions, as shown in Fig. 2. In this figure, E_1 is the open-circuit voltage of the input generator.

A simple calculation shows that Fig. 2 can be replaced by the more convenient form of Fig. 3, where the whole circuit is, in effect, completely separated into two parts, the ω_1 circuit and the ω_2 circuit.

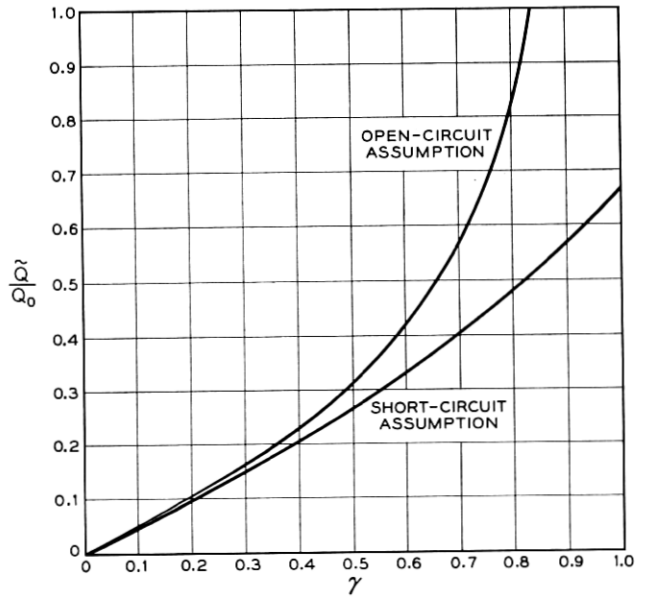

Fig. 1 — Q/Q_0 vs. γ.

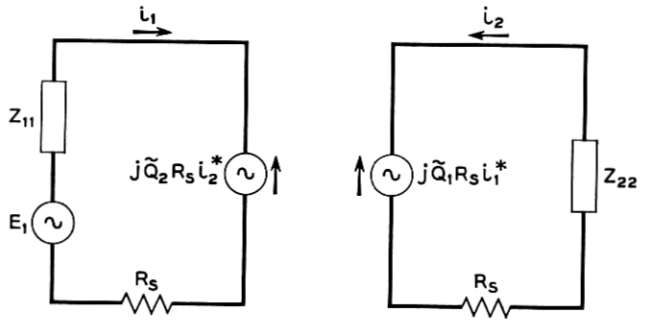

Fig. 2 — Circuit representation of lower sideband amplifier.

The real part of the input impedance of the diode at ω_1 is

$$R_s + \text{Re}\left(-\frac{\tilde{Q}_1\tilde{Q}_2 R_s^2}{R_s + Z_{22}^*}\right).$$

The largest magnitude of the negative resistance is obtained when Z_{22} is equal to zero, and the resistance is

$$R_s(1 - \tilde{Q}_1\tilde{Q}_2).$$

It is worth noting that when $\tilde{Q}_1\tilde{Q}_2$ becomes unity the diode no longer shows negative resistance and the amplifier ceases to show gain.

III. MINIMUM NOISE FIGURE FOR LARGE GAIN

From Fig. 3 the output power at the idler frequency is easily calculated. The result is

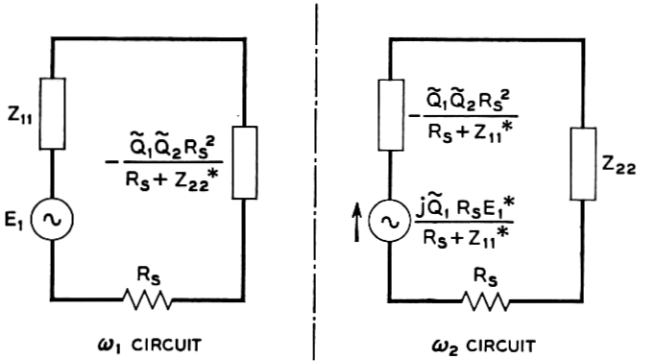

Fig. 3 — Equivalent circuit of lower sideband amplifier

$$P_{21} = \frac{\frac{R_L}{R_s^2}\tilde{Q}_1^2 \mid E_1 \mid^2}{\left|\left(1 + \frac{Z_{11}^*}{R_s}\right)\left(1 + \frac{Z_{22}}{R_s}\right) - \tilde{Q}_1\tilde{Q}_2\right|^2}, \tag{12}$$

where R_L is the load resistance and is a part of Z_{22}.

Since the available power of the source is

$$P_{av} = \frac{\mid E_1 \mid^2}{4R_g}, \tag{13}$$

where R_g is the internal resistance of the generator, the gain becomes

$$G_{21} = \frac{4\frac{R_gR_L}{R_s^2}\tilde{Q}_1^2}{\left|\left(1 + \frac{Z_{11}^*}{R_s}\right)\left(1 + \frac{Z_{22}}{R_s}\right) - \tilde{Q}_1\tilde{Q}_2\right|^2}. \tag{14}$$

Equation (14) is the gain of the amplifier whose input is at ω_1 and output at ω_2.

The noise voltage in the ω_1 circuit is given by

$$\mid e_{n_1} \mid^2 = 4kB(T_gR_g + T_1R_1 + T_sR_s), \tag{15}$$

where $R_g + R_1$ is the real part of Z_{11}; k is the Boltzmann constant; B is the bandwidth; and T_g, T_1, and T_s are the temperatures of R_g, R_1, and R_s, respectively.

Substituting (15) in place of $\mid E_1 \mid^2$ in (12), the noise output due to this noise voltage becomes

$$N_{21} = \frac{4kB(T_gR_g + T_1R_1 + T_sR_s)\frac{R_L}{R_s^2}\tilde{Q}_1^2}{\left|\left(1 + \frac{Z_{11}^*}{R_s}\right)\left(1 + \frac{Z_{22}}{R_s}\right) - \tilde{Q}_1\tilde{Q}_2\right|^2}. \tag{16}$$

Similarly, the noise output at ω_2 produced by noise sources in the ω_2 circuit is found to be†

$$N_{22} = \frac{4kB(T_LR_L + T_2R_2 + T_sR_s)\frac{R_L}{R_s^2}\left|1 + \frac{Z_{11}^*}{R_s}\right|^2}{\left|\left(1 + \frac{Z_{11}^*}{R_s}\right)\left(1 + \frac{Z_{22}}{R_s}\right) - \tilde{Q}_1\tilde{Q}_2\right|^2}, \tag{17}$$

where $R_L + R_2$ is the real part of Z_{22} and T_L and T_2 are the temperatures

† The assumption is made that the gain of the amplifier is large. If it is small, a more elaborate calculation is necessary.

of R_L and R_2 respectively. Upon combining (14), (16), and (17), the noise figure of the amplifier becomes

$$F_2 = \frac{N_{21} + N_{22}}{G_{21} k T_g B} = 1 + \frac{T_1 R_1 + T_s R_s}{T_g R_g} + \frac{T_L R_L + T_2 R_2 + T_s R_s}{T_g R_g} \frac{\left| 1 + \frac{Z_{11}^*}{R_s} \right|^2}{\tilde{Q}_1^2} . \quad (18)$$

Equation (18) is the noise figure of the lower sideband idler output amplifier. In a similar manner, one can calculate the gain and noise figure of the amplifier whose input and output are both at ω_1 but separated by means of a circulator:†

$$G_{11} \simeq \frac{4 \frac{R_g^2}{R_s^2} \left| 1 + \frac{Z_{22}^*}{R_s} \right|^2}{\left| \left(1 + \frac{Z_{11}}{R_s} \right) \left(1 + \frac{Z_{22}^*}{R_s} \right) - \tilde{Q}_1 \tilde{Q}_2 \right|^2} , \quad (19)$$

$$F_1 \simeq 1 + \frac{T_1 R_1 + T_s R_s}{T_g R_g} + \frac{T_L R_L + T_2 R_2 + T_s R_s}{T_g R_g} \frac{\tilde{Q}_2^2}{\left| 1 + \frac{Z_{22}^*}{R_s} \right|^2} . \quad (20)$$

For both cases, the large-gain condition is given by

$$\left(1 + \frac{Z_{11}}{R_s} \right) \left(1 + \frac{Z_{22}^*}{R_s} \right) = \left(1 + \frac{Z_{11}^*}{R_s} \right) \left(1 + \frac{Z_{22}}{R_s} \right) = \tilde{Q}_1 \tilde{Q}_2 , \quad (21)$$

where we have made use of the fact that $\tilde{Q}_1 \tilde{Q}_2$ is a real quantity. Substituting (21) into (18) and (20), the identical noise figure expression is obtained for both the lower sideband idler output and circulator-type amplifier, namely,

$F =$

$$1 + \frac{T_1 R_1 + T_s R_s}{T_g R_g} + \frac{T_L R_L + T_2 R_2 + T_s R_s}{T_g R_g} \frac{\omega_1}{\omega_2} \frac{R_g + R_1 + R_s}{R_L + R_2 + R_s} . \quad (22)$$

The following discussion, therefore, holds equally well for both cases.

Let us assume first that T_L is equal to T_s and that T_2 is not smaller than T_s. Under these conditions, using the high-gain condition (21) in conjunction with (22), it can be shown that R_g must be as large as possible to minimize the noise figure. Using (21), this requires that R_1, $R_L + R_2$, and the reactive components of Z_{11} and Z_{22} must all be as small as possible.

† The assumption is made that the gain of the amplifier is large. If it is small, a more elaborate calculation is necessary.

When

$$R_L = R_1 = R_2 = \text{Im } Z_{11} = \text{Im } Z_{22} = 0,\dagger \tag{23}$$

(21) becomes

$$1 + \frac{R_g}{R_s} = \tilde{Q}_1\tilde{Q}_2\,, \tag{24}$$

and the noise figure expression simplifies to give the minimum value of

$$F_m = 1 + \frac{\frac{T_s}{T_g}}{\tilde{Q}_1\tilde{Q}_2 - 1}\left(1 + \frac{\omega_1}{\omega_2}\,\tilde{Q}_1\tilde{Q}_2\right). \tag{25}$$

Equation (25) is the minimum noise figure of a lower sideband amplifier with a fixed idler frequency under the assumption of only a series-resistance parasitic element. Equation (25) is a function of ω_2, and there is an optimum idler frequency for which a minimum is obtained. Using the relation

$$\tilde{Q}_2 = \frac{\omega_1}{\omega_2}\,\tilde{Q}_1 \tag{26}$$

and (25), the smallest noise figure $F_{m,m}$ (i.e. optimized impedances and optimized idler frequency) is given by

$$F_{m,m} = 1 + 2\,\frac{T_s}{T_g}\left(\frac{1}{\tilde{Q}_1^{\,2}} + \frac{1}{\tilde{Q}_1}\sqrt{1 + \frac{1}{\tilde{Q}_1^{\,2}}}\right), \tag{27}$$

when

$$\frac{\omega_2}{\omega_1} = \sqrt{1 + \tilde{Q}_1^{\,2}} - 1. \tag{28}$$

In Fig. 4, F_m is plotted versus $\tilde{Q}_1$ for several different values of ω_2/ω_1 under the condition $T_s = T_g$. Fig. 5 gives the corresponding plot of $F_{m,m}$ versus $\tilde{Q}_1$. The optimum value for ω_2/ω_1 versus $\tilde{Q}_1$ is shown in Fig. 6.

IV. IDLER LOAD REFRIGERATION

In the noise figure expression, (25), we have assumed that $T_L = T_s$ and concluded that, to obtain a low noise figure, the idler load re-

† For the lower sideband idler output amplifier, if $R_L = 0$, the numerator of (14) becomes zero. However, by a suitable adjustment of the denominator, we may still have large gain for the limiting case of $R_L \to 0$.

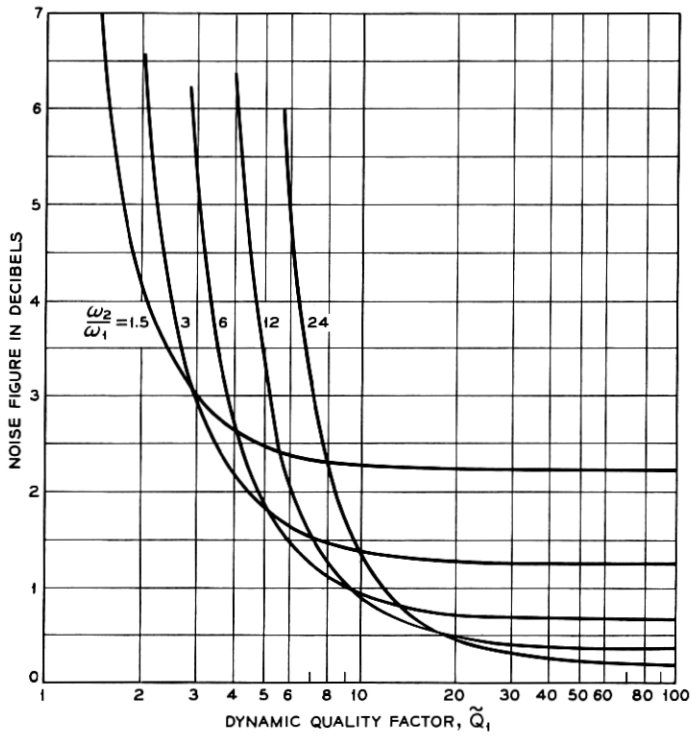

Fig. 4 — Minimum noise figure F_m of lower sideband amplifier with fixed idler frequency.

sistance R_L should be as small as possible. If $T_L < T_s$,† however, one may expect to obtain a further improvement in the noise figure for a fixed idler frequency by properly adjusting the load resistance. We shall now examine this possibility, but again under the assumption that T_2 is not smaller than T_s. From (22), under the condition of constant R_L, the value of the noise figure becomes small when R_g becomes large. Because of the large-gain condition (21), the maximum in R_g is obtained when

$$R_1 = R_2 = \text{Im } Z_{11} = \text{Im } Z_{22} = 0. \tag{29}$$

We shall assume that (29) is satisfied. The condition $R_L = 0$ is now not necessarily the case for the minimum noise figure, since the last

† There are two ways of characterizing T_L. In the treatment presented here, it is used to signify the black body emission back into the circuit (see Section III). It has a second description in terms of the noise figure of the output load which implies $T_L \gg T_s$, but this is not the present definition of T_L.

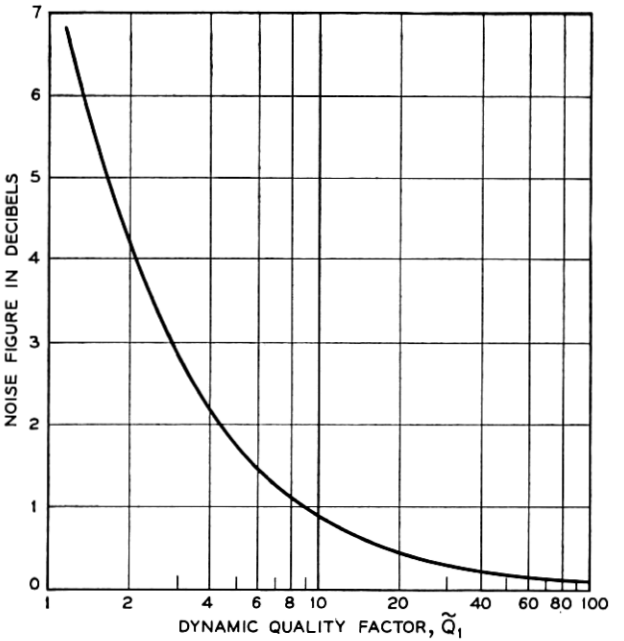

Fig. 5 — Minimum noise figure $F_{m,m}$ of lower sideband amplifier with optimized idler frequency or minimum noise figure F_m of upper sideband up-converter.

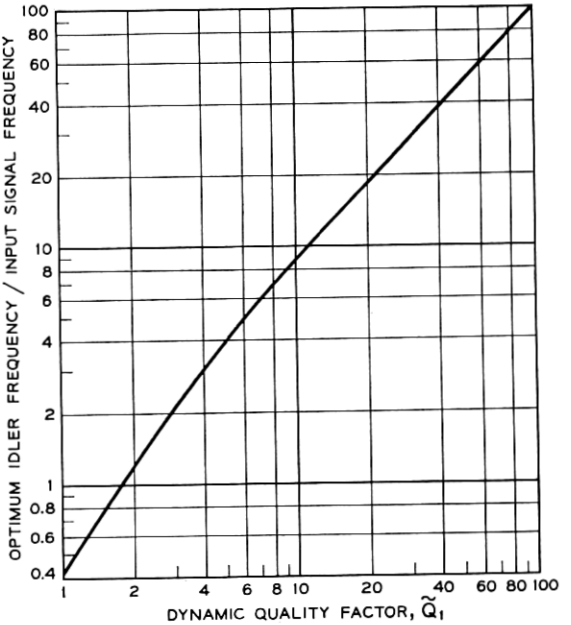

Fig. 6 — Normalized optimum idler frequency.

term of (22) can decrease when R_L increases, provided that $T_L < T_s$. If $T_L < T_s$, from (21) and (22) together with the above assumption, the conditions for the minimum noise figure are given by

$$R_g = R_s \sqrt{1 + \left(\frac{\omega_2}{\omega_1} + \frac{T_L}{T_s}\right) \frac{\tilde{Q}_1\tilde{Q}_2}{1 - \frac{T_L}{T_s}}} \tag{30}$$

and

$$R_L = R_s \left[\frac{\tilde{Q}_1\tilde{Q}_2}{1 + \sqrt{1 + \left(\frac{\omega_2}{\omega_1} + \frac{T_L}{T_s}\right) \frac{\tilde{Q}_1\tilde{Q}_2}{1 - \frac{T_L}{T_s}}}} - 1 \right]. \tag{31}$$

The noise figure is expressed as

$$F = 1 + \frac{T_s}{T_g} \left[\frac{T_L}{T_s} \frac{\omega_1}{\omega_2} + 2 \frac{1 - \frac{T_L}{T_s}}{\tilde{Q}_1^2} + 2 \frac{1}{\tilde{Q}_1} \sqrt{\left(1 - \frac{T_L}{T_s}\right)\left(1 + \frac{T_L}{T_s} \frac{\omega_1}{\omega_2} + \frac{1 - \frac{T_L}{T_s}}{\tilde{Q}_1^2}\right)} \right]. \tag{32}$$

To obtain a real and positive value of R_L in (31), the condition

$$\frac{\frac{\omega_2}{\omega_1} + 1}{1 - \frac{T_L}{T_s}} < \tilde{Q}_1\tilde{Q}_2 - 1 \tag{33}$$

must be satisfied. If this is not the case, the minimum noise figure (25) is obtained when $R_L = 0$, and is consistent with the results of the previous theory; this will be so when $\tilde{Q}_1\tilde{Q}_2$ is close to unity, or when the load temperature is close to the diode temperature. On the other hand, if $T_L > T_s$, we see from (22) that the noise figure decreases as the idler load R_L is reduced, and the minimum noise figure is again given by (25) when $R_L = 0$. Next, we shall check whether or not the condition (33) is satisfied for the optimum idler frequency.

From (26) and (28), the condition (33) becomes

$$\frac{1}{1 - \frac{T_L}{T_s}} < 1. \tag{34}$$

Because $0 \leqq T_L \leqq T_s$, the condition (34) is not satisfied. This shows

that the effort to get further improvement in noise figure by cooling the idler load resistance proves to be useless after adjusting the idler frequency to the optimum. Finally, if we make $T_L = 0$ in (32), then we have exactly the same expression as (27). In this case, the condition (33) becomes

$$\frac{\omega_2}{\omega_1} < \sqrt{1 + \tilde{Q}_1^2} - 1. \tag{35}$$

Comparing (35) with (28), we conclude that, as long as the idler frequency is less than the optimum, the minimum noise figure obtainable with a zero-temperature idler load is equal to the best that is obtainable by optimizing the idler frequency.

As an example, taking $\omega_1/\omega_2 = 3$, the curves F versus T_L/T_s are shown in Fig. 7 for several different $\tilde{Q}$'s under the condition $T_g = T_s$.

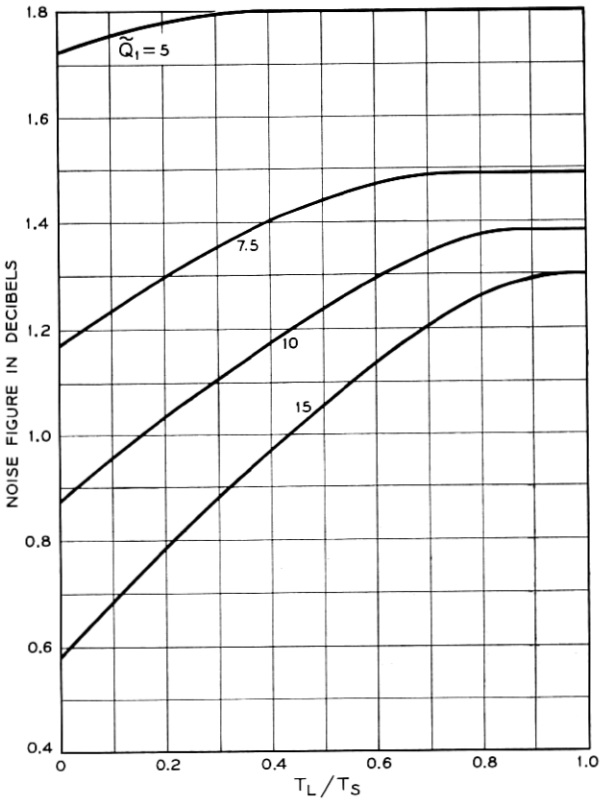

Fig. 7 — Effect of idler load refrigeration. Idler-to-signal frequency ratio of 3 is used for this calculation.

V. DOUBLE SIDEBAND OPERATION

In double sideband operation, the signal is introduced in a substantially symmetrical manner about half the pump frequency so that signal and noise are present both at ω_1 and at ω_2. Therefore, assuming $Z_{11} \simeq Z_{22}$, $\omega_1 \simeq \omega_2$, and $T_L \simeq T_g$, the noise figure expression, derived after some manipulation, is

$$F = \frac{N_{11} + N_{12}}{kTB(G_{11} + G_{12})} = 1 + \frac{T_1R_1 + T_sR_s}{T_gR_g}. \tag{36}$$

The large-gain condition remains the same as (21). To minimize the noise figure, R_g must be as large as possible and hence

$$R_1 = R_2 = \text{Im } Z_{11} = \text{Im } Z_{22} = 0. \tag{37}$$

Then, (21) becomes

$$1 + \frac{R_g}{R_s} = \tilde{Q}. \tag{38}$$

From (36), (37), and (38), the minimum noise figure F_m is obtained. One finds

$$F_m = 1 + \frac{T_s}{T_g}\frac{1}{\tilde{Q} - 1}. \tag{39}$$

The curve F_m versus $\tilde{Q}$ for $T_s = T_g$ is shown in Fig. 8.

VI. COMPARISON WITH EXPERIMENT

A considerable number of noise figure measurements have been made for double sideband operation at 6 kmc. Some of these results (Table I) are plotted in Fig. 9 as a function of the usual quality factor as measured at zero bias voltage.†

The circles indicate the results for zero bias operation, and the triangles indicate those for biased operation with optimum adjustment. The pump power and the amplifier circuit were adjusted for optimum noise conditions. The gain of the amplifier was maintained constant at 16 db.

The theoretical noise figure curves for several different γ's are also drawn in the same figure. The values for γ given in brackets correspond to the short-circuit assumption; those without brackets correspond to the open-circuit assumption.

It is worth noting that the noise figures measured for the same kind of diode are found in the vicinity of the same γ curve. For example,

† A technique for measuring $\tilde{Q}$, and the comparison between the measured noise figures and the measured values of $\tilde{Q}$, will be published in the near future.

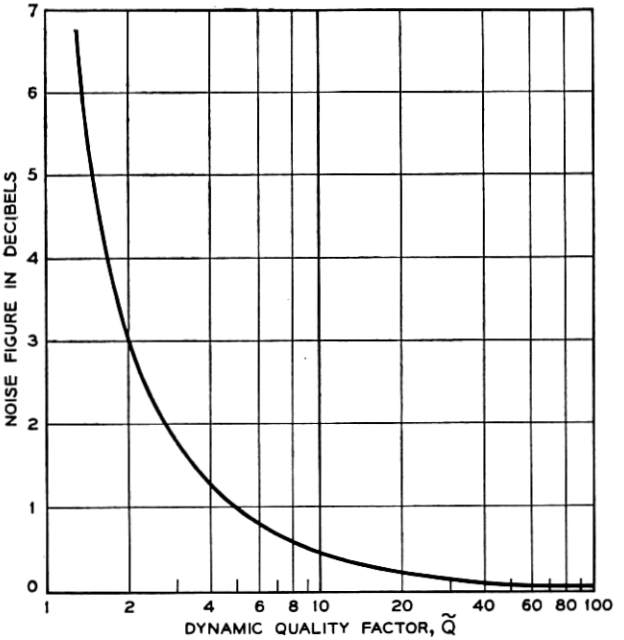

Fig. 8 — Minimum noise figure F_m of lower sideband degenerate amplifier.

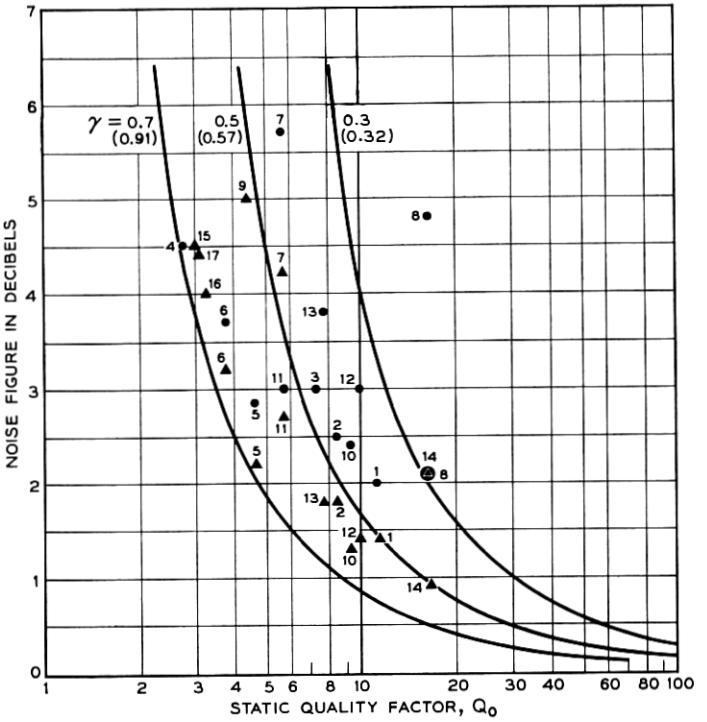

Fig. 9 — Measured results for noise figure of various diodes. Circles indicate the results for zero bias operation, triangles are for biased operation. Solid lines

TABLE I—MEASURED RESULTS OF NOISE FIGURES FOR VARIOUS DIODES

Diode Number	Material	Q	F for no bias (db)	F for bias (db)
1	silicon	11.2	2.0	1.4
2	silicon	8.5	2.5	1.8
3	silicon	7.4	3.0	—
4	silicon	2.74	4.5	—
5	silicon	4.74	2.87	2.2
6	silicon	3.88	3.7	3.2
7	germanium	5.78	5.7	4.2
8	germanium	16.65	4.3	2.1
9	silicon	4.4	—	5.0
10	silicon	9.3	2.4	1.3
11	silicon	5.85	3.0	2.7
12	gallium arsenide	10.0	3.0	1.4
13	gallium arsenide	7.7	3.8	1.8
14	gallium arsenide	16.7	2.1	0.9
15	germanium-gold	3.0	—	4.5
16	germanium-gold	3.3	—	4.0
17	germanium-gold	3.1	—	4.4

numbers 1, 2, 3, 10, and 11 are silicon p-n junction diodes, and their points are a little above the curve $\gamma = 0.5$ for zero bias operation and a little below the same curve for biased operation. Numbers 12, 13, and 14 are gallium arsenide diodes, and their noise figures are found along the $\gamma = 0.3$ curve for no bias operation and a little below the $\gamma = 0.5$ curve for biased operation. For germanium-gold bonded diodes, numbers 15, 16, and 17, the corresponding value of γ is 0.65 for biased operation.

It should be mentioned that the effective Q of the diode at the operating point is not the same as that measured at zero bias. This is because the capacitance of the diode is nonlinear and the pump voltage is swept over a wide range. Therefore, the average capacitance of the diode depends on the amplitude of the pump power and the characteristic of the capacitance. Thus, the values of γ corresponding to the measured noise figures do not give a direct indication of the γ used in the calculations. However, the difference is expected to be small. Also it should be mentioned that the Q's of the diodes were in fact measured at 1 kmc, and then calculated for the operating frequency of 6 kmc using a relation similar to (26).

VII. EQUIVALENT CIRCUIT FOR THE UP-CONVERTER

For the upper sideband up-converter, the diode junction is characterized by relationships similar to those for the lower side-band amplifier; that is,

$$\begin{bmatrix} e_1 \\ e_2 \end{bmatrix} = \begin{bmatrix} \frac{1}{j\omega_1 K_0} & \frac{1}{j\omega_2(2K_1)} \\ \frac{1}{j\omega_1(2K_1)} & \frac{1}{j\omega_2 K_0} \end{bmatrix} \begin{bmatrix} i_1 \\ i_2 \end{bmatrix} \tag{40}$$

when making the open-circuit assumption for the unwanted frequencies, and

$$\begin{bmatrix} i_1 \\ i_2 \end{bmatrix} = \begin{bmatrix} j\omega_1 C_0 & j\omega_1 \frac{C_1}{2} \\ j\omega_2 \frac{C_1}{2} & j\omega_2 C_0 \end{bmatrix} \begin{bmatrix} e_1 \\ e_2 \end{bmatrix} \tag{41}$$

when making the short-circuit assumption for the unwanted frequencies. From these equations, in a similar manner to that of Section II, the equivalent circuit of Fig. 10 is obtained for both cases.

From this equivalent circuit, the gain and noise figure are found to be

$$G = \frac{4 \frac{R_g R_L}{R_s^2} \tilde{Q}_1^2}{\left| \left(1 + \frac{Z_{11}}{R_s}\right)\left(1 + \frac{Z_{22}}{R_s}\right) + \tilde{Q}_1 \tilde{Q}_2 \right|^2}, \tag{42}$$

$$F = 1 + \frac{T_s R_s + T_1 R_1}{T_g R_g} + \frac{T_s R_s + T_2 R_2}{T_g R_g} \left| 1 + \frac{Z_{11}}{R_s} \right|^2 \frac{1.}{\tilde{Q}_1^2}. \tag{43}$$

To obtain (43), we have disregarded the noise contribution of R_L. The reasoning here follows from the conventional definition of the noise

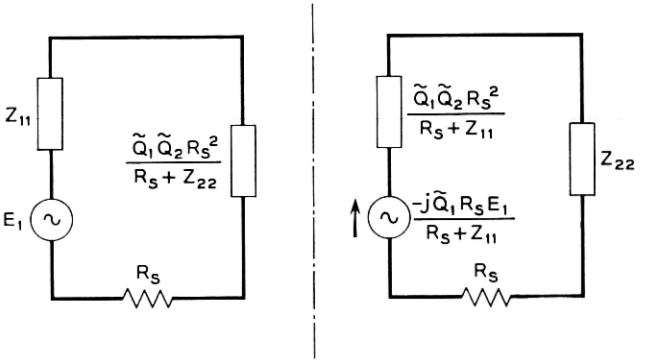

Fig. 10 — Equivalent circuit of upper sideband up-converter.

figure which is identified with a particular stage and does not include the noise contribution of the following stage. Here, R_L is taken as the input impedance of the second stage. This is quite different from the negative-resistance amplifier discussed before, where the noise power from the load is also amplified and is, therefore, taken into account as extra noise attributable to the amplification process.

VIII. MINIMUM NOISE FIGURE

Equation (43) shows that the minimum noise figure is obtained when $1 + (Z_{11}/R_s)$ is real and R_1 and R_2 are as small as possible. Therefore, by adjusting the circuit so that

$$R_1 = 0, \quad R_2 = 0, \quad 1 + \frac{Z_{11}}{R_s} = 1 + \frac{R_g}{R_s}, \tag{44}$$

(43) becomes

$$F = 1 + \frac{T_s}{T_g}\left[\frac{R_s}{R_g} + \frac{R_s}{R_g}\left(1 + \frac{R_g}{R_s}\right)^2 \frac{1}{\tilde{Q}_1^2}\right]. \tag{45}$$

Minimizing F with respect to R_g, the noise figure becomes

$$F_m = 1 + 2\frac{T_s}{T_g}\left(\frac{1}{\tilde{Q}_1^2} + \frac{1}{\tilde{Q}_1}\sqrt{1 + \frac{1}{\tilde{Q}_1^2}}\right) \tag{46}$$

when

$$R_g = R_s\sqrt{1 + \tilde{Q}_1^2} \equiv R_s L. \tag{47}$$

Comparing (46) with (27), we find that the minimum noise figure is equal to that of the lower sideband amplifier when this is used with the optimum idler frequency or with a zero temperature idler load.

The condition for the minimum noise figure is given by (47). There is a further degree of freedom in the resistance of the load, which does not appear in the noise expression (45). This degree of freedom is resolved by choosing R_L for maximum gain. The gain under the assumption of minimum noise figure is

$$G = \frac{4\dfrac{R_g R_L}{R_s^2}\tilde{Q}_1^2}{\left|\left(1 + \dfrac{R_g}{R_s}\right)\left(1 + \dfrac{R_L}{R_s}\right) + \tilde{Q}_1\tilde{Q}_2\right|^2}. \tag{48}$$

Maximizing G with respect to R_L, the gain becomes

$$G = \frac{\frac{\omega_2}{\omega_1}}{\left(1 + \frac{1}{\tilde{Q}_1\tilde{Q}_2} + \frac{1}{\tilde{Q}_1\tilde{Q}_2}\sqrt{1 + \tilde{Q}_1^2}\right)\left(1 + \frac{1}{\sqrt{1 + \tilde{Q}_1^2}}\right)} \tag{49}$$

when the output is matched, i.e.,

$$R_L = R_s\left(1 + \frac{\tilde{Q}_1\tilde{Q}_2}{1 + \frac{R_g}{R_s}}\right) \equiv R_s M . \tag{50}$$

Equation (49) is thus the maximum gain under the restriction of minimum noise figure. When $\tilde{Q}_1$ and $\tilde{Q}_2$ become large, the gain approaches ω_2/ω_1, as is to be expected. The curves F versus $\tilde{Q}_1$ and G versus $\tilde{Q}_1$ are shown in Figs. 5 and 11 respectively. Fig. 12 shows L versus $\tilde{Q}_1$ and M versus $\tilde{Q}_1$ for several different values of ω_2/ω_1.

IX. MAXIMUM GAIN

Next we shall calculate the maximum gain condition irrespective of the minimum noise figure condition imposed earlier.

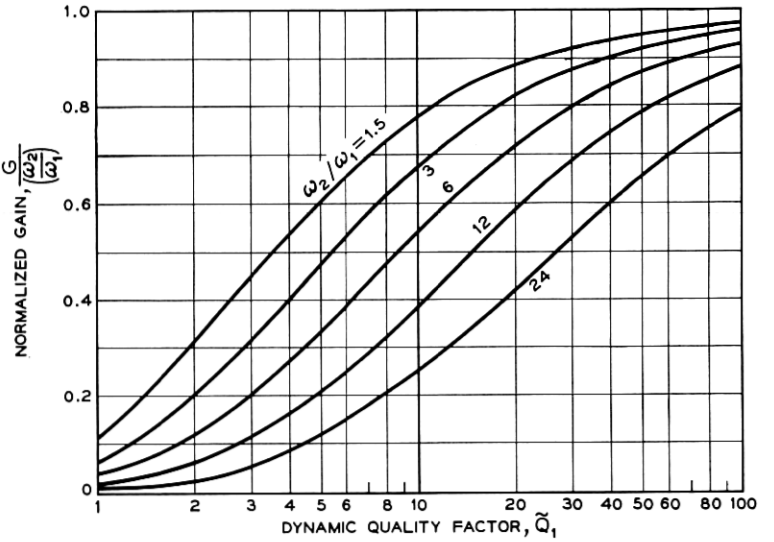

Fig. 11 — Normalized gain of upper sideband up-converter under minimum noise figure condition.

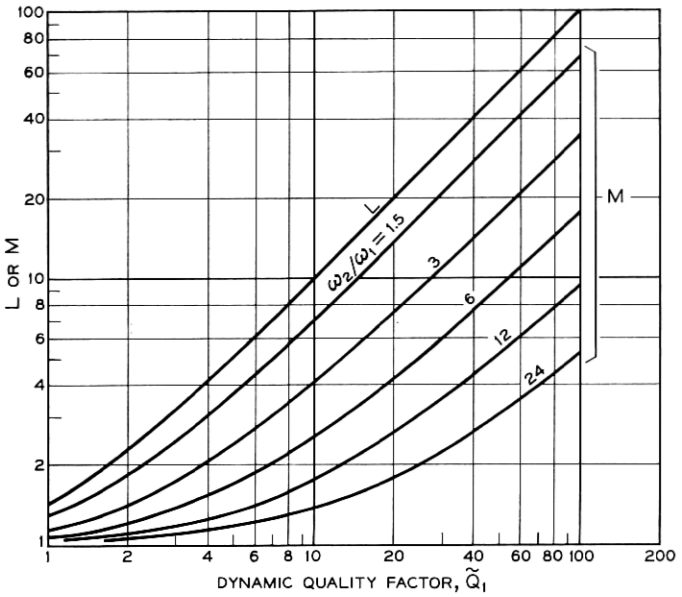

Fig. 12 — L and M vs. Q_1.

From (42), assuming R_g and R_L to be constant, the largest gain is provided by the conditions that Z_{11} and Z_{22} are real and that R_1 and R_2 vanish. We therefore only need to investigate the expression (48). Upon maximizing the right-hand side of (48) with respect to R_g and R_L, the gain becomes

$$G = \frac{\omega_2}{\omega_1}\frac{\sqrt{1 + \tilde{Q}_1\tilde{Q}_2} - 1}{\sqrt{1 + \tilde{Q}_1\tilde{Q}_2} + 1} = \frac{\omega_2}{\omega_1}\frac{K - 1}{K + 1} \tag{51}$$

when

$$R_g = R_L = R_s\sqrt{1 + \tilde{Q}_1\tilde{Q}_2} \equiv R_sK. \tag{52}$$

The noise figure under this condition is

$$\begin{aligned} F &= 1 + \frac{T_s}{T_g}\left(\frac{1}{\sqrt{1 + \tilde{Q}_1\tilde{Q}_2}} + \frac{\omega_1}{\omega_2}\frac{1}{\sqrt{1 + \tilde{Q}_1\tilde{Q}_2}}\frac{\sqrt{1 + \tilde{Q}_1\tilde{Q}_2} + 1}{\sqrt{1 + \tilde{Q}_1\tilde{Q}_2} - 1}\right) \\ &= 1 + \frac{T_s}{T_g}\left(\frac{1}{K} + \frac{\omega_1}{\omega_2}\frac{1}{K}\frac{K + 1}{K - 1}\right). \end{aligned} \tag{53}$$

If $\tilde{Q}_1\tilde{Q}_2$ is large, K is large, G approaches ω_2/ω_1, and F tends to unity, as

is to be expected. The curves F versus $\tilde{Q}_1$, G versus $\tilde{Q}_1$ and K versus $\tilde{Q}_1$ are shown in Figs. 13, 14, and 15.

X. MINIMUM OVER-ALL NOISE FIGURE

In the previous discussions of the upper sideband up-converter, only the noise figure of the up-converter was considered and no attention was paid to the following stage. However, in a practical system, the over-all noise figure is more important than that of the preamplifier itself. This is especially so when the gain of the preamplifier is low, or the over-all noise figure is much higher than that of the preamplifier alone. We shall therefore consider in this section the over-all noise figure.

As discussed in the previous section, the condition for the minimum noise figure of the up-converter does not coincide with that for the maximum gain. Therefore, the best over-all noise performance is ob-

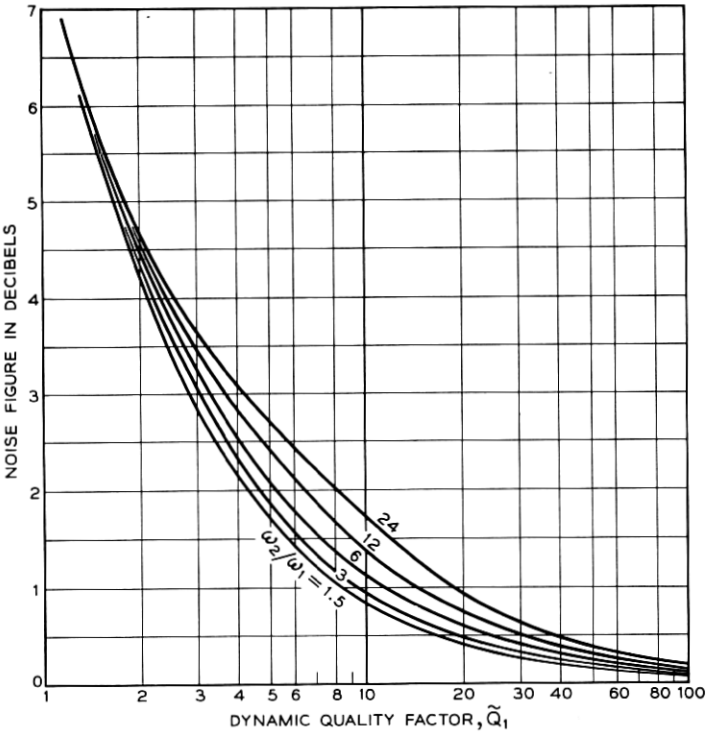

Fig. 13 — Noise figure of upper sideband up-converter under maximum gain condition.

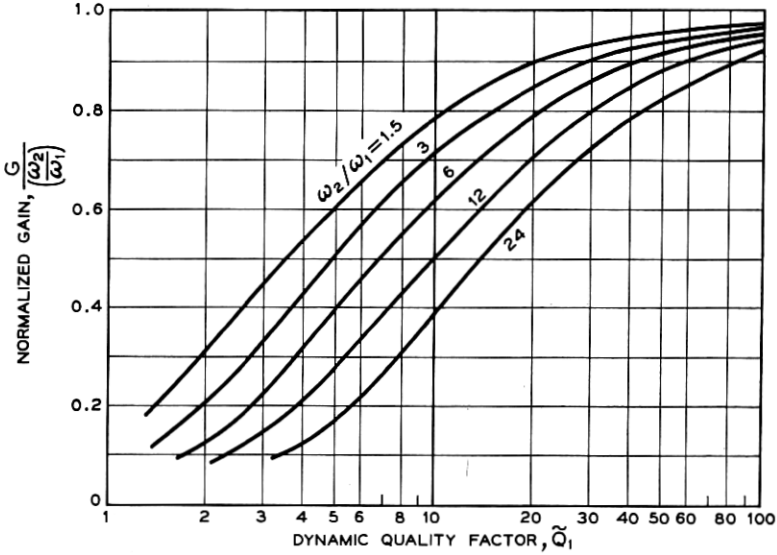

Fig. 14 — Normalized maximum gain of upper sideband up-converter.

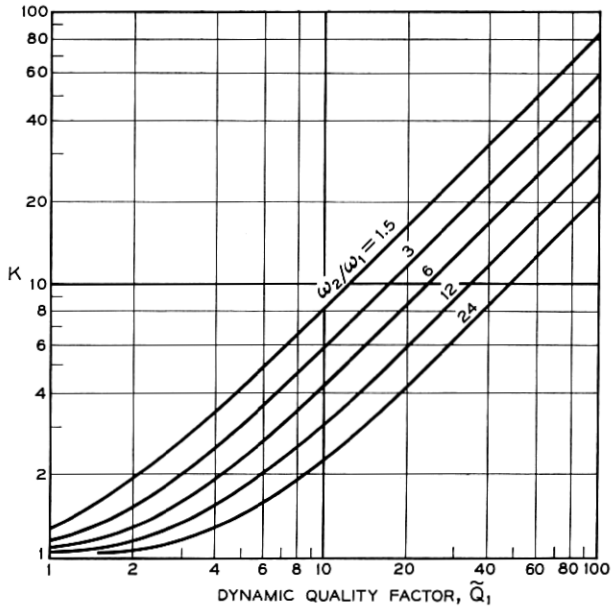

Fig. 15 — K vs. Q_1 .

tained neither at the minimum noise figure condition nor with maximum gain.

The noise figure of the second stage depends on the input impedance. In this discussion, however, we shall assume that the second-stage input impedance is kept constant by connecting an isolator in front of it. Thus, the noise figure of the second stage is defined regardless of any possible mismatch in the output impedance of the up-converter.

The over-all noise figure is given by

$$F_0 = F_1 + \frac{F_2 - 1}{G_1}, \tag{54}$$

where F_1 is the noise figure of the up-converter including the isolator, G_1 is the gain, and F_2 is the noise figure of the second stage.

Since the best over-all noise figure is obtained when F_1 is small and G_1 is large, we have only to investigate the case where Z_{11} and Z_{22} are real and R_1 and R_2 are equal to zero.

From (45), (48), and (54), the over-all noise figure becomes

$$\begin{aligned} F_0 = 1 + \frac{T_s}{T_g}\left[\frac{1}{L_0} + \frac{1}{L_0}\frac{(1+L_0)^2}{\tilde{Q}_1^2}\right] \\ + \frac{T_L}{T_g}\frac{\left[(1+L_0)(M_0-1) - \tilde{Q}_1^2\frac{\omega_1}{\omega_2}\right]^2}{4L_0M_0\tilde{Q}_1^2} \\ + (F_2 - 1)\frac{\left[(1+L_0)(1+M_0) + \tilde{Q}_1^2\frac{\omega_1}{\omega_2}\right]^2}{4L_0M_0\tilde{Q}_1^2}, \end{aligned} \tag{55}$$

where

$$R_g \equiv R_s L_0, \quad R_L \equiv R_s M_0. \tag{56}$$

Minimizing F_0 with respect to M_0, the optimum M_0 is given by

$$M_0 = 1 + \frac{\omega_1}{\omega_2}\frac{\tilde{Q}_1^2}{1+L_0}. \tag{57}$$

This is the same condition as (50). Under this condition, the optimum value L_0 is found to be

$$L_0 = \tilde{Q}_1\left[\frac{1}{\tilde{Q}_1^2} + \frac{\frac{T_s}{T_g} + \frac{\omega_1}{\omega_2}(F_2 - 1)}{\frac{T_s}{T_g} + F_2 - 1}\right]^{\frac{1}{2}}. \tag{58}$$

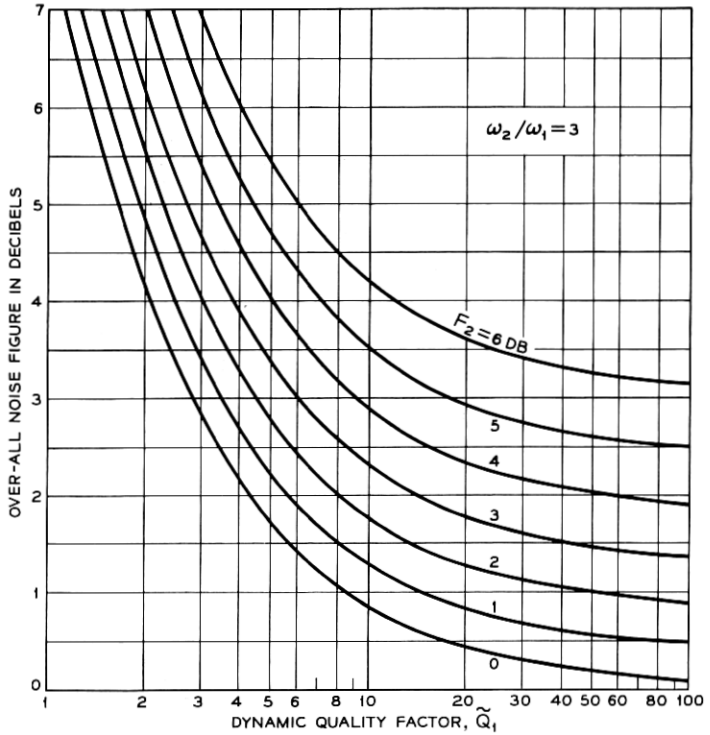

Fig. 16 — Over-all noise figure F_0. Output-to-signal frequency ratio of 3 is used for this calculation.

If we make $F_2 = 1$, (58) becomes

$$L_0 = \sqrt{1 + \tilde{Q}_1^2},$$

which is the same as (47), the condition for the minimum noise figure. If we make $F_2 \to \infty$, (57) and (58) become

$$M_0 = \sqrt{1 + \tilde{Q}_1\tilde{Q}_2},$$

$$L_0 = \sqrt{1 + \tilde{Q}_1\tilde{Q}_2}.$$

These are the maximum gain conditions which appear in (52). Therefore, as expected, when the second stage has a very poor noise figure, the up-converter should be adjusted for the maximum gain condition, while it must be at the minimum noise figure condition if the second stage noise figure is close to unity.

From (55), (57), and (58), the minimum over-all noise figure is given by

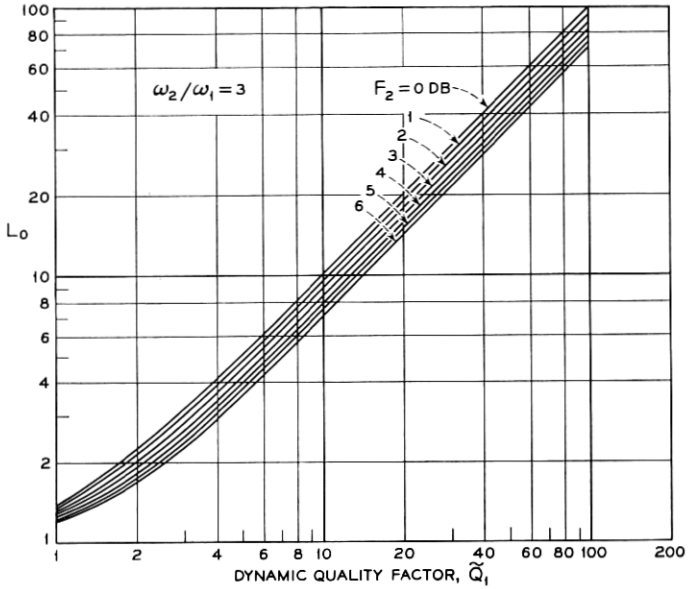

Fig. 17 — L_0 vs. Q_1 .

$$F_0 = 1 + \frac{2}{\tilde{Q}_1^2}\left(\frac{T_s}{T_g} + F_2 - 1\right) + \frac{\omega_1}{\omega_2}(F_2 - 1) + \frac{2}{\tilde{Q}_1}\sqrt{\left[\frac{T_s}{T_g} + \frac{\omega_1}{\omega_2}(F_2 - 1) + \frac{1}{\tilde{Q}_1^2}\left(\frac{T_s}{T_g} + F_2 - 1\right)\right]\left(\frac{T_s}{T_g} + F_2 - 1\right)}. \tag{59}$$

As an example, taking $T_s/T_g = 1$ and $\omega_2/\omega_1 = 3$, the curves F_0 versus $\tilde{Q}_1$, L_0 versus $\tilde{Q}_1$, and M_0 versus $\tilde{Q}_1$ are shown in Figs. 16, 17, and 18, respectively, to show the general tendency of the variations in these parameters.

XI. CONCLUSION

On the assumption that the series resistance of the diode is the only parasitic element, we have calculated the minimum noise figures for both the lower sideband and the upper sideband parametric amplifiers under various conditions. For each case, the noise figure is basically determined by the dynamic quality factor $\tilde{Q}$ of the diode. The larger $\tilde{Q}$ is, the lower is the noise figure which can be obtained. If the practically obtainable values of $\tilde{Q}$ are equal for different diodes, the same minimum noise figure is expected. Even for the static diode Q, i.e., Q_0 is very high, it is impossible to build a low-noise amplifier if the capacitance varia-

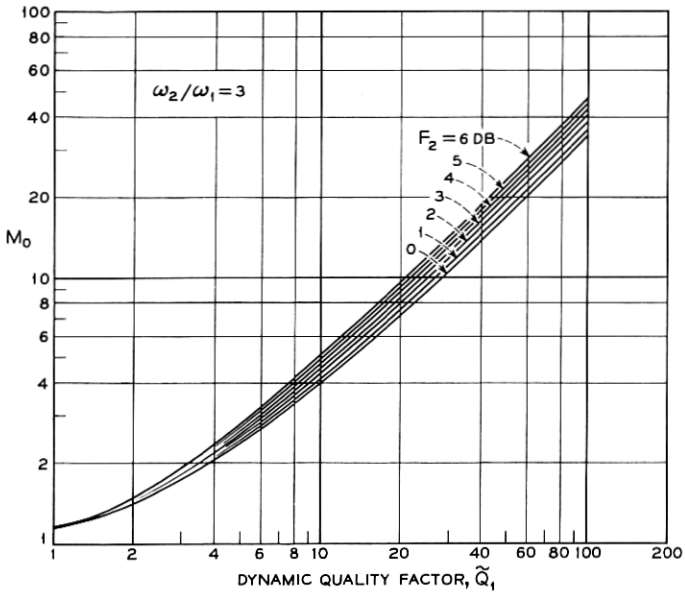

Fig. 18 — M_0 vs. $\tilde{Q}_1$.

tion is small. Therefore, we conclude that the dynamic quality factor $\tilde{Q}$ is more appropriate than Q_0 as a measure of the quality of a variable capacitance diode.

The identical noise figure expression is obtained for both the lower sideband idler output and the circulator-type amplifier, if the gain in each case is large. The minimum noise figure of the lower sideband amplifier for room-temperature operation is obtained when the idler load resistance approaches zero. For a given $\tilde{Q}_1$ there exists an optimum idler frequency at which the realizable noise figure is equal to the best that is obtainable with a zero temperature idler load.

The minimum noise figure of the upper sideband up-converter is equal to that of the lower sideband amplifier. Since the maximum gain of the upper sideband up-converter is limited by the ratio of output to input frequency, while the gain of the lower sideband amplifier is unlimited, a superior over-all noise figure is expected with the lower sideband amplifier.

XII. ACKNOWLEDGMENTS

Acknowledgments are due to H. Seidel and K. D. Bowers for stimulating discussions and helpful criticism in preparation of this manuscript.

APPENDIX

Stability Comparison for Two Different Types of Lower Sideband Amplifier

Since the lower sideband idler-output and circulator-type amplifiers give the same noise figure under the large-gain condition, the question of which is more stable arises. With large gain and minimum noise operation, the idler-output type is less stable than the circulator type. To see that this is so, consider the gain expressions (14) and (19). The major cause for instability comes from the denominator, since the two terms in the denominator almost cancel each other and a small variation of either term brings about a large variation in the gain. For instance, a small increase in the pump power can cause enough variation in $\tilde{Q}_1\tilde{Q}_2$ for the amplifier to break into oscillation. Similarly, a small change in the input impedance Z_{11} gives a large variation.

For a given gain, if the numerator is small, the cancellation of the two terms in the denominator must be more complete; in other words, the negative resistance effect must be more fully utilized, making the amplifier less stable. Thus, for the comparison of the stability of the two types, we only have to investigate the numerator of the gain expressions.

For the minimum noise figure,

$$R_g = R_s(\tilde{Q}_1\tilde{Q}_2 - 1),$$

$$R_L \to 0.$$

Hence we see at once that the idler-output type has the smaller numerator, making it the less stable amplifier.

Let us now consider the case where R_L is small but finite, i.e., where we accept some degradation in noise performance. The comparison should then be made between $R_g \simeq R_s\tilde{Q}_1\tilde{Q}_2$ and $R_L\tilde{Q}_1^2$, for $|\ 1 + (Z_{22}^*/R_s)\ |^2$ is approximately unity and $\tilde{Q}_1\tilde{Q}_2 \gg 1$. From this comparison, we find that $R_L/R_s > \omega_1/\omega_2$ is the approximate condition for the idler-output type to be the more stable. The noise figure does not change very rapidly when R_L/R_s changes a little from its optimum value of zero. In fact, the noise figure thus obtainable corresponds to a decrease in $\tilde{Q}_1\tilde{Q}_2$ by the factor of $R_s/(R_s + R_L)$. We therefore conclude that, when the ratio of the idler frequency to the signal frequency is large, the idler-output type can be made the more stable with only a small sacrifice in the noise figure.

There is still another type of operation, namely the transmission type, where the output load is directly coupled at the signal frequency. It can be shown in a way similar to the above discussion that, using this

scheme, it is never possible to achieve more stable operation than with the circulator type, and the obtainable noise figure is poorer than or at best equal to that of the circulator type.

It should be remarked that the major limitation in the bandwidth also comes from the denominator of the gain expression. The above argument therefore holds equally well for a bandwidth comparison.

The above discussion holds only for room-temperature operation. If load refrigeration is available (i.e., a cold isolator at the idler frequency), a different conclusion is reached; i.e., under certain conditions, it is possible to make the idler-output type more stable without a sacrifice in the noise figure.

REFERENCES

1. Leenov, D., Gain and Noise Figure of a Variable Capacitance Up-Converter, B.S.T.J., **37**, 1958, p. 989.
2. Haus, H. A., and Penfield, P., Jr., On the Noise Performance of Parametric Amplifiers, Internal Memorandum No. 19, Massachusetts Inst. of Technology, Cambridge, Mass.
3. Uenohara, M., Noise Consideration of the Variable Capacitance Parametric Amplifier, Proc. I.R.E., **48**, 1960, p. 169.
4. Kotzebue, K. L., Optimum Noise Performance of Parametric Amplifiers, Proc. I.R.E., **48**, 1960, p. 1324.
5. Knechtli, R. C., and Weglein, R. D., Low-Noise Parametric Amplifier, Proc. I.R.E., **48**, 1960, p. 1218.
6. Bloom, S., and Chang, K. K. N., Theory of Parametric Amplification Using Nonlinear Reactances, R.C.A. Rev., **18**, 1957, p. 578.
7. Rowe, H. E., Some General Properties of Nonlinear Elements. II — Small Signal Theory, Proc. I.R.E., **46**, 1958, p. 850.
8. Heffner, H., and Wade, G., Gain, Bandwidth and Noise Characteristics of the Variable Parameter Amplifier, J. Appl. Phys., **29**, 1958, p. 1321.